Magnetic-induction profile in a type-I superconductor by polarized-neutron reflectometry

M. P. Nutley*
Institut Laue-Langevin, 156X, 38042 Genoble CEDEX, France

A. T. Boothroyd and C. R. Staddon
Department of Physics, Clarendon Laboratory, University of Oxford, Parks Road, Oxford, OX1 3PU, United Kingdom

D. M^{c}K. Paul
Department of Physics, University of Warwick, Coventry, CV4 7AL, United Kingdom

J. Penfold
ISIS Science Division, Rutherford Appleton Laboratory, Chilton, Didcot, Oxon., OX11 0QX, United Kingdom
(Received 17 February 1994)

We have used the technique of polarized-neutron reflectometry to study the magnetic-induction profile just beneath the surface of a 1-μm-thick film of lead with the magnetic field applied parallel to the surface. The sample was maintained at a temperature of 1.5 K throughout the experiment, and the applied field H was varied from below H_c, the bulk critical field, up to the critical field for surface superconductivity, H_{c3}. From the measurements with the lead film in the bulk superconducting phase ($H<H_c$) we found that the spin-dependent reflectivity profiles are consistent with an exponential decay of magnetic induction with a penetration depth $\lambda=39\pm1$ nm. At higher applied fields ($H_c<H<H_{c3}$) we obtained information on the diamagnetism in the surface superconducting layer. We discuss the sensitivity of the measurements to the form of the magnetic-induction profile, in particular to nonlocal effects, and show that a good description of the surface diamagnetism, over the whole range of applied fields, can be achieved with the local Ginzburg-Landau theory if the Ginzburg-Landau parameter κ is allowed to vary with the applied field.

I. INTRODUCTION

When a magnetic field H is applied parallel to the surface of a type-I superconductor at a temperature below the superconducting transition temperature T_c the exclusion of magnetic flux from inside the sample can take place in two different ways, according to whether H is greater than, or less than, the bulk critical field H_c. If $H<H_c$ then the magnetic induction B vanishes everywhere except in a region of order the penetration depth λ beneath the surface. The application of higher fields ($H>H_c$) destroys the bulk superconductivity, and usually allows magnetic flux to penetrate the entire sample as for a normal metal. Under special circumstances, however, a superconducting layer may persist just below the surface, at a depth approximately equal to the coherence length ξ, and flux will be excluded to a certain extent from this region.

For this surface superconductivity to exist the applied field must be greater than H_c but less than the *surface critical field*, H_{c3}. Within the Ginzburg-Landau theory,[1] H_c and H_{c3} are related by[2]

$$H_{c3}=2.39\kappa H_c \ , \tag{1}$$

where $\kappa=\lambda/\xi$ is the Ginzburg-Landau parameter. With the requirement that H_{c3} be greater than H_c, it follows from Eq. (1) that κ must exceed 0.42 for the surface superconducting phase to be possible.

Although λ and ξ do indicate the characteristic length scales over which the magnetic induction in the bulk and surface superconducting phases vary, they do not, by themselves, define the actual shape of the magnetic-induction profile $B(z)$, which measures the value of the magnetic induction at a distance z beneath the surface of the superconductor. In the London limit, which applies to high-κ, type-II superconductors, the magnetic induction decays exponentially with depth,[3] $B(z)\sim\exp(-z/\lambda)$, and the profile is determined by one parameter, λ, alone. In general, however, $B(z)$ does not vary in a simple way with z. The evaluation of $B(z)$ for the surface superconducting layer can only be achieved by numerical solution of the equations describing the electrodynamic properties of the superconductor,[4] and for low-κ materials, especially type-I superconductors ($\kappa<1/\sqrt{2}$), the nonlocal relation between induced current density and magnetic induction[5] should also be taken into account. Theoretical calculations for the bulk superconducting phase have shown that the range of the magnetic-field penetration is increased by nonlocal effects, that the shape deviates from an exponential, and that under some circumstances the magnetic induction can actually change sign.[6,7] This sign reversal has been observed experimentally in tin.[8]

Tests of such calculations cannot be made from a knowledge of λ and ξ alone. Ideally, what is required is a set of experimental measurements of the full magnetic-induction profile $B(z)$ as a function of κ and H. The

most direct technique available that can provide information on $B(z)$ is polarized-neutron reflectometry (PNR).[9–11] The method works because the fraction of neutrons reflected specularly from a sample depends on the way in which the scattering potential varies normal to the surface, and because included in the potential is a magnetic term proportional to the difference between the internal and external magnetic induction. The scattering potential also contains a nonmagnetic part, proportional to the nuclear scattering length density, but it is possible to separate the nuclear and magnetic parts with polarized neutrons, since the nuclear potential is independent of the orientation of the neutron spin, whereas the magnetic interaction changes sign according to whether the neutrons are polarized parallel or antiparallel to the magnetic field.

The application of PNR to probe magnetic-field profiles in superconductors has been relatively recent, but a number of systems have been studied. The technique was used to determine the penetration depth of niobium[12] and of the high-T_c superconductor $YBa_2Cu_3O_7$,[13,14] and to investigate the surface superconducting layer in an alloy of lead and bismuth (0.8% Bi in Pb).[15] In this work we chose to use lead as the superconductor because it can exhibit the surface superconducting phase without the need for alloying. The use of a pure metal is simpler from the point of view of theory because in a "dirty" alloy the impurity atoms act as scattering centers that break up the coherence of the conduction-electron pairs. This introduces another length scale, the electron mean free path, and therefore greater complexity, into the problem.[5]

The aim of the work described in this paper was to investigate the magnetic-induction profile in lead both in the bulk and surface superconducting phases, and to compare the results with calculations derived from models for $B(z)$. Lead is a type-I superconductor with $T_c=7.2$ K and $H_c(0)\approx 6.4\times 10^4$ A/m (800 Oe) at absolute zero, so the conditions required for bulk and surface superconductivity are easily accessible to experiment. Some PNR measurements on pure lead have already been presented,[14,15] but these showed no indication of diamagnetism above H_c. This is because at the temperature the measurements were carried out, 4.4 K (Ref. 14) and 5.5 K (Ref. 15), $H_{c3}\approx H_c$ (Ref. 16) or, in other words, κ as defined by Eq. (1) is approximately 0.42, which is marginal for surface superconductivity. In pure lead, κ increases as the temperature decreases,[17] and so the surface superconductivity occurs only at temperatures less than 5.5 K. Our measurements were performed at 1.5 K, at which temperature $\kappa\approx 0.55$.

II. EXPERIMENTAL DETAILS

The lead film was deposited by evaporation onto an ion-cleaned, silicon substrate, which was cut from a polished single-crystal wafer. The area of the substrate was approximately 3×3 cm^2, and the thickness of the film was 1 μm as recorded by a quartz flux monitor positioned adjacent to the substrate during the evaporation process. Immediately after preparation, the sample was sealed under nitrogen inside a plastic bag for transportation. This precaution was taken because lead rapidly develops a surface oxide layer on exposure to air.

The neutron experiment took place on the CRISP reflectometer at the spallation neutron source, ISIS. A full description of the instrument is given elsewhere.[18] Here we summarize only those features particular to the operation of CRISP with polarized neutrons.[19]

The CRISP beamline views a liquid-hydrogen moderator, from which emerges a polychromatic beam of neutrons, pulsed at the source frequency of 50 Hz. The neutron beam is spin-polarized by reflection from a cobalt-titanium mirror, and the polarization state is reversed when required in a Drabkin, two-coil, nonadiabatic spin flipper. Two slit apertures upstream of the sample serve to collimate the neutron beam, and the sample itself is glued onto an adjustable platform inside a pumped ^{4}He cryostat. An electromagnet external to the cryostat applies a horizontal magnetic field parallel to the surface of the sample. The specularly reflected neutrons are counted in a single ^{3}He gas detector situated 1.75 m away from the sample.

In the time-of-flight method, the angle θ of the neutron beam incident on the sample is fixed, and the reflectivity is recorded as a function of neutron wavelength λ_n, which is given by the flight time from the target to the detector. The reflectivity depends only on the component of the scattering vector normal to the surface, $Q_z=(4\pi/\lambda_n)\sin\theta$, and because of the intrinsic narrowness of the neutron pulse the resolution in Q_z is dominated by the divergence of the incident beam. During the present experiment θ was set to 0.3°, a value which gave us an accessible range of Q_z that covered the part of the reflectivity curve most sensitive to the variation in magnetic induction in the superconductor. The nominal divergence $\Delta\theta$ [full width at half maximum (FWHM) of the equivalent Gaussian distribution], defined by the slit openings, was 0.017°. As will be discussed later, the values for these angle parameters used in the analysis were allowed to vary slightly to match the measured reflectivity profiles.

An important aspect of this study was that as many as possible of the experimental parameters were kept constant throughout the experiment. Thus, only one sample was used, the same instrument configuration was maintained, and the sample temperature was 1.5 K during every run. The only variable that was changed during the course of the experiment was the applied magnetic field. By minimizing the number of variables in this way we hoped to achieve the maximum sensitivity to relative changes in the field profile in the superconductor from run to run, particularly with regard to differences above and below H_c.

III. ANALYSIS

A single PNR run yields the reflectivities for neutrons polarized parallel (R^+) and antiparallel (R^-) to the applied magnetic field, as a function of wavelength or, more physically, Q_z. Total reflection of neutrons ($R^+=R^-=1$) occurs at wavelengths above the critical wavelength, but for shorter wavelengths the reflectivities fall vary rapidly. The difference between R^+ and R^- is

greatest just below the critical wavelength, and this is the region of the curve most sensitive to the magnetic-induction profile. As with the phase problem in crystallography, it is not possible to derive $B(z)$ directly from the measured reflectivities. Instead, the information is retrieved by means of a calculation of R^+ and R^- from a model for $B(z)$. Such a calculation can be performed by a numerical integral transform,[20] or by a matrix method in which $B(z)$ is made into a discrete function of z through the hypothetical subdivision of the sample into a large number of planes of constant magnetic induction.[10] The latter approach, which is an adaptation of the problem of the propagation of electromagnetic radiation through stratified media,[20] is the one which we have adopted. In order to avoid generating spurious oscillations in the calculated reflectivity due to the discrete sampling of $B(z)$ we chose the size of the elements, Δz, to be much smaller than any of the other length scales that affect the reflectivity, and typically Δz was between 0.5 and 1 nm.

There are several corrections which need to be incorporated into a reflectivity calculation in order to achieve a realistic simulation of the experimental conditions. In our case, three extra factors were important: the divergence of the incident neutron beam; the local roughness of the surface; and the existence of a nonsuperconducting lead-oxide layer on the surface of the films. We took account of the incident-beam divergence by averaging the reflectivity over a Gaussian distribution of incident angles with a full width at half maximum of $\Delta\theta$, and included the effect of surface roughness in the conventional way via a factor $I(\lambda_n)$ which depends on the neutron wavelength and incident angle, and which resembles a Debye-Waller factor.[21,22] $I(\lambda_n)$ includes a parameter $\langle z_D^2 \rangle$ that may be interpreted as the mean-squared deviation of points on the surface from their average position. Lead oxidizes very rapidly upon exposure to air, and the oxide layer that forms on the surface affects the reflectivity. Unfortunately, we were not able to analyze the oxide layer on the same sample as used in the neutron experiment because the surface was damaged by condensation when the film was removed from the cryostat after the experiment. Instead, we based our assumptions concerning this layer on x-ray studies[23] of lead films evaporated onto silicon single crystal substrates under similar conditions to ours. These have shown that orthorhombic PbO is the oxide type that forms, and that the thickness of the surface layer Δz_{PbO} is typically 5 nm. We found that the calculated reflectivities were not particularly sensitive to Δz_{PbO} in the region near the critical edge where the reflectivity is most spin dependent, and so in order to reduce the number of fitting parameters we fixed Δz_{PbO} at 5 nm, a value consistent with the x-ray analysis and which also gave a good description of the part of the reflectivity curves well below the critical wavelength. Similar experiences with the surface oxide layer were reported in Ref. 15.

Although, in principle, the angle and divergence of the incident neutron beam are defined by the geometry of the spectrometer they are still uncertain to some degree, and in practice we found that θ and $\Delta\theta$ were best treated together with $\langle Z_D^2 \rangle$ as fitting parameters, to be obtained from the measured reflectivities. Ideally, these three parameters should have remained constant throughout the entire experiment, in which case they could have been obtained once and for all from a single reflectivity measurement under conditions where the lead was in the normal, metallic state (e.g., $T > T_c$). In reality, however, the action of refilling the cryostat with ^{4}He caused minute changes in the sample alignment which were manifest as small shifts in the critical edge of the reflectivity spectra. We felt it prudent, there, *in the first instance* to treat θ, $\Delta\theta$, and $\langle z_D^2 \rangle$ as fitting parameters, to be obtained for each run from the best fit of the model to the measured reflectivities.

Ideally, this surface characterization should have been carried out with the lead film in the normal state where the reflectivity is spin independent. Heating the sample above T_c for every field, however, would have compromised our original intention to maintain the sample conditions as constant as possible, and would also have been costly in neutron time. Instead, we adopted the simpler, but approximate, approach of fitting the calculated *spin-independent* reflectivity to the average of the two *spin-dependent* reflectivities R^+ and R^- measured at $T = 1.5$ K. This procedure is valid as long as the flipping ratio, R^+/R^-, is close to unity.

A typical example of such a fit is given in Fig. 1, which shows the spin-averaged reflectivity measured in a field of 5.6×10^4 A/m (700 Oe). The results of the fit to this curve were $\theta = 0.293° \pm 0.0005°$, $\Delta\theta = 0.023° \pm 0.0011°$, and $\langle z_D^2 \rangle = (10.0 \pm 0.8)$ nm. The curve calculated without the 5-nm surface layer of PbO is also shown in Fig. 1 to demonstrate how the reflectivity is modified by the oxide layer. Considering the results for all the different fields, we found a range of θ values from 0.293° to 0.303°, but only small variations in $\Delta\theta$ and $\langle z_D^2 \rangle$ that were comparable with the statistical error in any one fit. For the remainder of the analysis, therefore, we used $\Delta\theta = 0.023°$

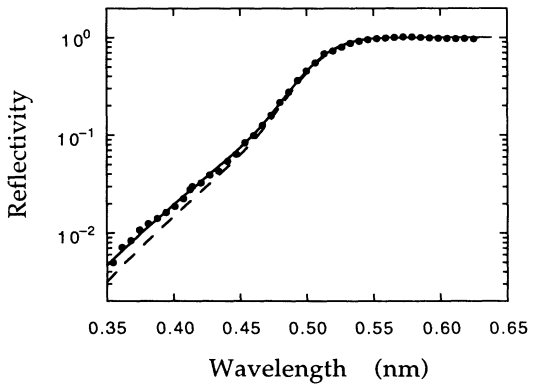

FIG. 1. The spin-averaged reflectivity of a 1-μm film of lead on a silicon substrate measured at a temperature of 1.5 K and in an applied magnetic field of 5.6×10^4 A/m (700 Oe). The continuous line is a model of the reflectivity, calculated for an incident angle of 0.293°, an angular divergence of 0.023° (FWHM), a surface roughness of 10 nm, and a 5-nm-thick surface layer of PbO. The broken line is calculated the same way but without the surface oxide layer.

and $\langle z_D^2 \rangle = 10$ nm as fixed parameters, but allowed θ to vary. Further fine tuning of the individual θ values took place during the next stage of the analysis when the spin-dependent reflectivities were considered.

IV. RESULTS

A. The bulk superconducting phase ($H < H_c$)

Figure 2 shows the reflectivities for the two polarization states measured in an applied magnetic field of 6.0×10^4 A/m (750 Oe), which is just below H_c for the sample temperature of 1.5 K. The difference between R^+ and R^- is clearly visible for neutron wavelengths close to 0.5 nm, just below the critical edge. This difference is more easily visualized on a plot of the flipping ratio R^+/R^-, as shown in Fig. 3 for the same data as in Fig. 2. The characteristic feature of the flipping ratio, data is a minimum centered just below the critical edge. The depth of this minimum was found to scale approximately with applied field for $H < H_c$, and as a result, the most accurate information on the magnetic induction was gained from measurements in which H was just below H_c.

Notwithstanding the possibility of nonlocal corrections, which will be discussed later, the most likely approximation to the magnetic-induction profile is the exponential decay law that emerges from the Londons' theory:

$$B(z) = \mu_0 H \exp(-z/\lambda) . \quad (2)$$

To test this model for $B(z)$ we fitted all the data sets measured with applied fields below H_c to the calculated spin-dependent reflectivities and flipping ratios, using Eq. (2) to describe the magnetic-induction profile. In these fits, only the penetration depth λ and the incident angle θ were allowed to vary, while the other surface parameters were fixed at the values obtained from the fits to the spin-averaged reflectivity and given in the preceding section. The continuous lines in Figs. 2 and 3 depict the best fit to the data measured at a field of 6.0×10^4 A/m, and in Fig. 4 we have magnified the region around the minimum and drawn the theoretical curves corresponding to penetration depths of 37 and 41 nm. These represent the acceptable limits within which the penetration depth might lie for this particular field. Similar bounds were obtained for all but the two lowest fields, for which the diamagnetic signals were too weak to yield an accurate value for λ.

Taking into consideration all of the five runs performed with fields less than H_c, we conclude that an exponential model for the magnetic-induction profile with penetration depth $\lambda = (39 \pm 1)$ nm describes the results of this experiment very well. The penetration depth showed no dependence on field within experimental error. Figure 5 summarizes the complete set of measurements for the bulk superconducting phase, together with calculations of the flipping ratios at each field for a constant penetration depth of 39 nm.

We turn next to the possibility of observing nonlocal effects in the PNR data. The work of Sommerhalder and Thomas[6] and of Halbritter[7] has predicted that for materials with low κ the induction profile will deviate from the

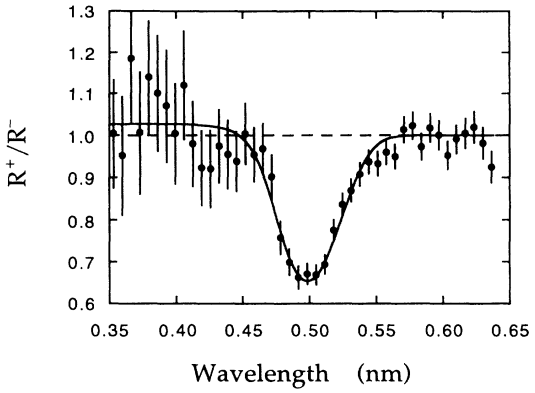

FIG. 3. The flipping ratio, R^+/R^-, for the data shown in Fig. 2.

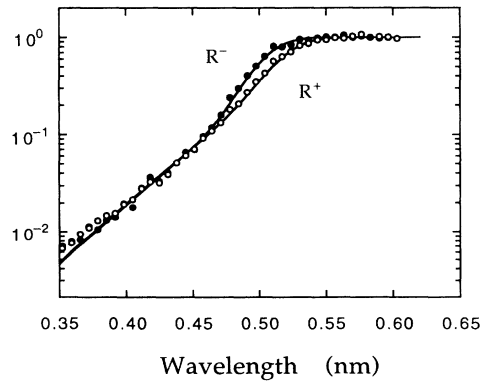

FIG. 2. The spin-dependent reflectivities R^+ and R^- measured in an applied magnetic field of 6.0×10^4 A/m (750 Oe). The continuous lines are the reflectivities calculated for the two polarization states, with the same instrumental and surface parameters as in Fig. 1, and an exponential decay of magnetic induction with a penetration depth of 39 nm.

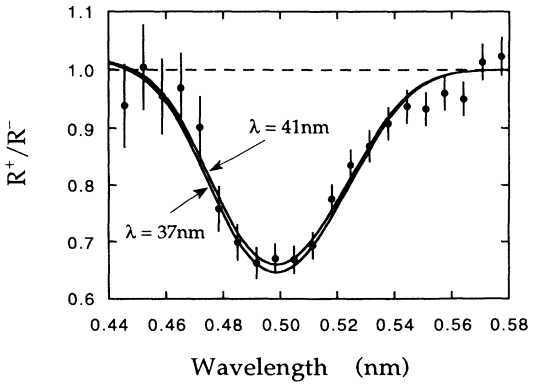

FIG. 4. An enlargement of the central portion of Fig. 3 with calculated curves corresponding to $\lambda = 37$ and 41 nm. These are the limits of uncertainty in λ for this data.

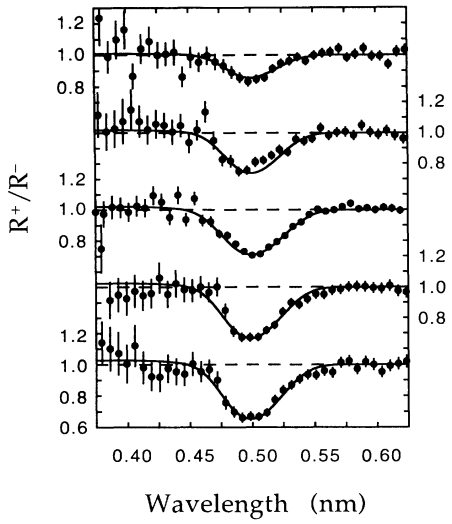

FIG. 5. The flipping ratios measured at a temperature of 1.5 K at five different values of the applied magnetic field in the bulk superconducting phase ($H < H_c$). The theoretical curves have all been calculated from a model which assumes the induction profile decays exponentially with a penetration depth $\lambda = 39$ nm. The instrumental and surface roughness parameters are the same for each calculated curve, and are as in Fig. 1. The values of the applied fields (in units of 10^4 A/m) are, from top to bottom, 2.0, 4.0, 4.8, 5.6, and 6.0.

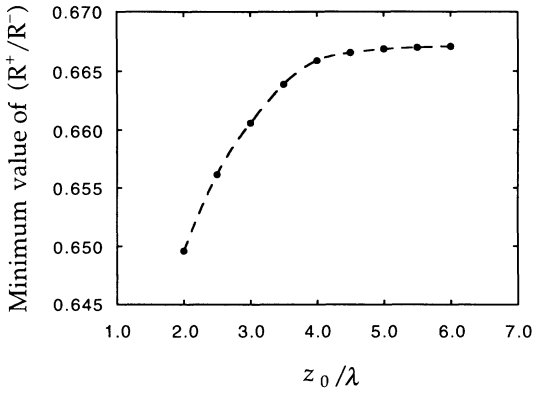

FIG. 6. Investigation of the possible influence of nonlocal effects on the flipping ratios. The plot shows how the minimum value of the flipping ratio changes when the exponential model induction profile is made to undergo an abrupt sign reversal at a depth z_0. Such sign reversals in $B(z)$ are known to occur in nonlocal superconductors when $z_0/\lambda \geq 4$, but this demonstration shows that the effect is too small to be detected by PNR.

exponential decay of Eq. (2) and, more specifically, that a sign reversal will occur at a certain distance beneath the surface which becomes smaller as κ decreases. For lead, the calculations predict the sign reversal to occur at a depth of $\sim 5.5\lambda$, with a largest negative value for the induction of $\sim 0.1\%$ of its value of the surface. These effects are very small indeed, and it is not surprising, therefore, that the exponential decay model is adequate to describe the present data within the experimental accuracy.

Although not manifest in our PNR data from lead, nonlocal effects could perhaps have a measurable influence on the flipping ratios with more extreme type-I superconductors, in which the sign reversal is nearer to the surface and the amplitude of the negative field maximum is greater. To investigate this possibility we have considered an approximate field profile in which $B(z)$ abruptly changes sign at a distance z_0 beneath the surface, and evaluated the spin-dependent reflectivities for different values of z_0. For this exercise we used the parameters appropriate to the present lead sample, $\theta = 0.30°$, $\Delta\theta = 0.023°$, $\langle z_D^2 \rangle = 10$ nm, and $\lambda = 39$ nm, and considered an applied field of 4.8×10^4 A/m. We found that varying z_0 affected the depth of the minimum in the flipping ratio curve, but did not noticeably change its shape. To illustrate the size of the effect, we plot in Fig. 6 the minimum flipping ratio as a function of the ratio z_0/λ. This figure shows that the flipping ratios are virtually insensitive to the sign reversal if it occurs at a depth greater than 4λ. The calculations of Halbritter[7] indicated that for *no value* of κ does the sign reversal occur much closer to the surface than 4λ and we conclude, therefore, that in its present form the technique of PNR *cannot* detect nonlocal corrections to the exponential decay of magnetic induction in the bulk superconducting phase.

B. The surface superconducting phase ($H_c < H < H_{c3}$)

The transition from bulk to surface superconductivity as H increases caused an abrupt change in the relationship between the spin-dependent reflectivities. Below H_c, the difference between R^+ and R^- increased with the applied field, as can be seen on Fig. 5, whereas above H_c, this trend was reversed. Following Ref. 15, we represent the field dependence of R^+ and R^- by the integral I_p of the polarization (also known as the spin asymmetry), $P = (R^+ - R^-)/(R^+ + R^-)$, over the normal component of the scattering vector, Q_z:

$$I_P = \int_0^\infty P(Q_z) dQ_z \ . \tag{3}$$

The values of I_p obtained from the reflectivity data are plotted against the applied magnetic field in Fig. 7. At low fields, I_p varies in proportion to the applied field, but between 6.0×10^4 A/m and 6.2×10^4 A/m there is a sudden drop in I_p, followed by a more steady decrease with extrapolates to zero at an applied field of approximately 8.1×10^4 A/m. Figure 7 closely resembles the equivalent plot in Ref. 15, for a Pb (0.8% Bi) alloy, which also showed a sharp drop in I_p followed by a residual signal at higher fields. The residual signal arises from the surface superconducting layer, and a comparison of Fig. 7 with the I_p data shown in Ref. 15 for pure lead measured at a temperature of 5.5 K, which shows no residual signal above H_c, confirms that in lead the surface superconductivity can only exist at temperature below 5.5 K. From Fig. 7 we estimate the critical fields for bulk and surface superconductivity at 1.5 K to be $H_c = (6.1 \pm 0.1) \times 10^4$ A/m [(765±10)Oe] and $H_{c3} = (8.1 \pm 0.3) \times 10^4$ A/m

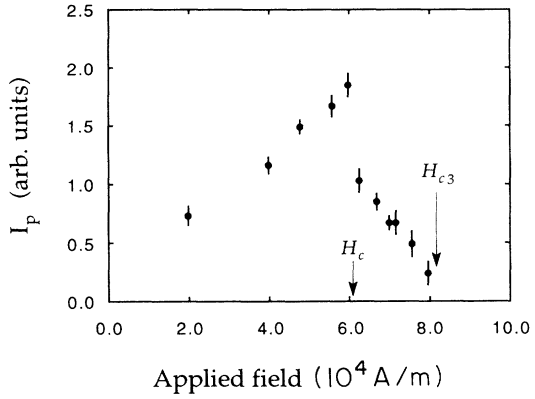

FIG. 7. The integral of the polarization, I_p, as defined in Eq. (3), plotted against the applied magnetic field. The critical fields H_c and H_{c3} at the working temperature of 1.5 K are indicated.

[(1020±30)Oe] and hence, from Eq. (1), we obtain $\kappa=0.56\pm0.02$.

The flipping ratio data from the surface superconducting phase, an example of which is given in Fig. 8 for a field of 6.7×10^4 A/m (840 Oe), very much resembles that from the bulk phase, with the only noticeable difference being a slight shift of the minimum of the curve towards larger wavelengths. Once again, the only way to extract information about the magnetic-induction profile for the surface superconducting layer is via a theoretical model for $B(z)$.

To our knowledge, the spatial profile of the diamagnetism in the surface superconducting layer has only ever been studied by solution of the nonlinear Ginzburg-Landau (GL) equations.[4] These calculations are necessarily inexact because the GL theory is only strictly valid in the local limit, i.e., for extreme type-II superconductors, and for temperatures near to T_c, but it nevertheless provides a useful and simple means by which an approximate form for $B(z)$ can be obtained.

In attempting to apply the GL theory to the present results we immediately encountered a problem. In order to solve the two nonlinear GL equations to find $B(z)$ as a function of the applied field we need values for two out of the four variables κ, λ, H_c, and H_{c3}, the other two being constrained within GL theory by Eq. (1) and by the relation[24]

$$\kappa=2\sqrt{2}\pi\frac{\mu_0 H_c\lambda_{\rm eff}^2}{\phi_0}\ , \tag{4}$$

where $\lambda_{\rm eff}$ is the GL effective penetration depth, and ϕ_0 is the flux quantum. Unfortunately, if we take $\lambda_{\rm eff}=\lambda$, and use the values of λ, H_c, and H_{c3} directly measured in this experiment, then Eqs. (1) and (4) do not yield the same result for κ: Eq. (1) gives $\kappa=0.56\pm0.02$ and Eq. (4) gives $\kappa=0.500\pm0.025$. In other words, the experimental values of the penetration depth and the critical fields for lead are not consistent with the GL theory.

In order to proceed with the GL theory, one or more of the experimental parameters had to be allowed to vary outside the experimental error. Concentrating on just the most accurately determined data set, that measured at an applied field of 6.7×10^4 A/m (see Fig. 8), we assumed first of all the value $\kappa=0.56$ derived from Eq. (1) with the measured H_c and H_{c3}, and set $\lambda_{\rm eff}$ to whatever value was required to satisfy Eq. (4). We then solved the GL equations numerically for $B(z)$ using the same method as Felici and Gray,[4] and calculated the spin-dependent reflectivities and flipping ratio with the same surface roughness and beam divergences parameters as obtained earlier from the analysis of the bulk superconducting phase. The resulting curve was a very poor fit to the measured flipping rations.

Next, we repeated the calculation assuming $\kappa=0.50$, as derived from Eq. (4) with the observed values of H_c and $\lambda_{\rm eff}=\lambda$. This approach yielded a much better fit to the data measured at $H=6.7\times10^4$ A/m, but when applied to the data taken at higher fields it increasingly underestimated the amount of surface diamagnetism. It is easy to see why this should be, as the value of H_{c3} predicted by Eq. (1) is significantly less than the field at which the diamagnetic signal actually vanished in practice. In other words, the surface diamagnetism extends to higher fields than predicted by the GL theory with $\kappa=0.50$.

It was apparent, therefore, that the GL magnetic-induction profile worked well at a *particular* value of the applied field, but that it was not able to describe the reflectivity data for *all* applied fields between H_c and H_{c3} with a single set of parameters. To illustrate the level of agreement which can be obtained with the GL theory, we have drawn on Fig. 8 the best fit achieved with H_c fixed at its experimental value, κ allowed to vary slightly from 0.50, and $\lambda_{\rm eff}$ tied to H_c and κ by Eq. (4). Figure 9 shows the corresponding magnetic-induction profile. The quality of the fit was very sensitive to κ, as shown in Fig. 10, which is an enlargement of the same data as in Fig. 8 but with theoretical curves corresponding to $\kappa=0.497$ and 0.501.

Although a theory is no longer meaningful if the so-called constants in the equations have to be varied in order to achieve a satisfactory description of a set of obser-

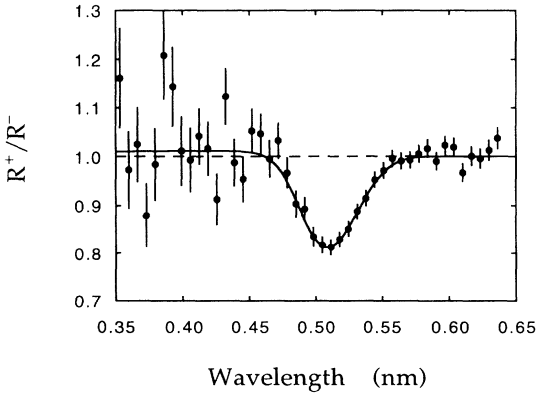

FIG. 8. Flipping ratios obtained from the surface superconducting layer of lead at a temperature of 1.5 K and in an applied field of 6.7×10^4 A/m (840 Oe). The continuous line is calculated from the GL theory induction profile with $\kappa=0.499$ and $\lambda_{\rm eff}=\lambda=39$ nm, and with instrumental and surface parameters the same as in Fig. 1.

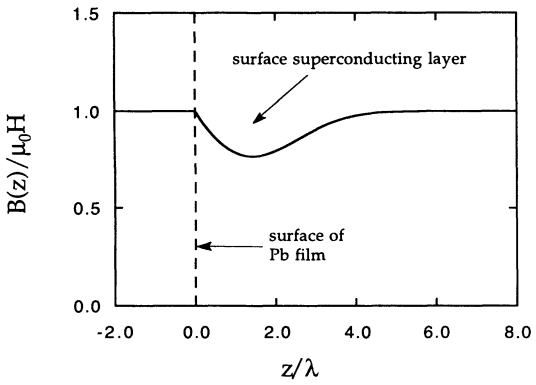

FIG. 9. The induction profile calculated from the GL theory that gives rise to the calculated flipping ratios in Fig. 8.

vations, we nevertheless felt that it might be possible to gain some insight into the failure of the GL theory, and also, perhaps, to establish a useful, empirical method to "patchup" the theory, if fits to all of the data sets could be achieved by allowing κ to vary with field but keeping the same fixed value of H_c and constrain λ_{eff} to satisfy Eq. (4) [note that this approach explicitly violates Eq. (1) except when $H=H_{c3}$]. The fitted data sets are shown in Fig. 11, and the values of $\kappa(H)$ that give the best fit at each field are plotted in Fig. 12. $\kappa(H)$ remains approximately constant at 0.50 for fields between H_c, and $\sim 7.2\times10^4$ A/m, then increases towards 0.56 at $H=H_{c3}$ the latter limit being determined, as of necessity, by the requirement that the diamagnetic signal vanishes the value of κ which satisfied Eq. (1).

V. DISCUSSION

We will begin by comparing the superconducting constants of lead obtained in this work with literature values from other techniques. From the variation of the integrated polarization with field, Fig. 7, we determined the bulk critical field at 1.5 K to be $H_c=(6.1\pm0.1)\times10^4$

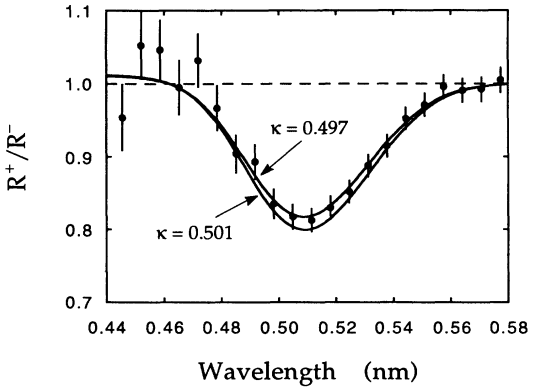

FIG. 10. An enlargement of the central portion of Fig. 8 but with calculated curves corresponding to $\kappa=0.497$ and 0.501. This illustrates the sensitivity of the flipping ratios to small variations in κ.

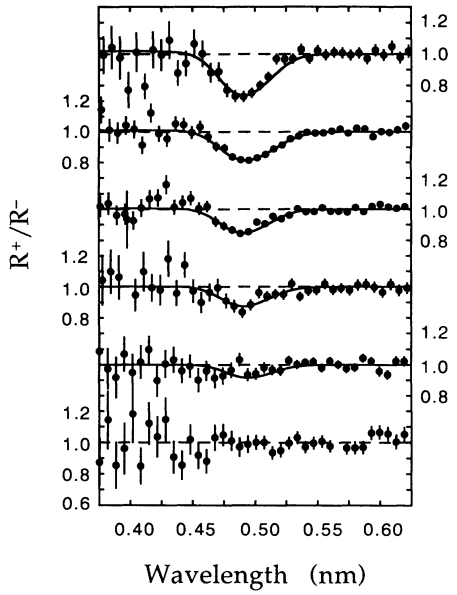

FIG. 11. The flipping ratios measured at a temperature of 1.5 K at six different values of the applied magnetic field in the surface superconducting phase ($H_c<H<H_{c3}$). The theoretical curves have all been calculated from the induction profiles derived from the GL theory with κ treated as a variable parameter. The instrumental and surface roughness parameters are the same for each calculated curve, and are as in Fig. 1. The values of the applied fields (in units of 10^4 A/m) are, from top to bottom, 6.25, 6.7, 7.0, 7.2, 7.6, and 8.0.

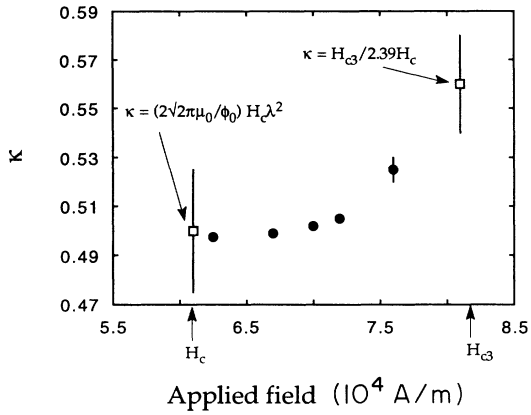

FIG. 12. The solid circles are the values of κ required in the GL theory to achieve the fits to the experimental flipping ratios shown in Fig. 11 with H_c fixed at the experimental value of 6.1×10^4 A/m. The small error bars reflect the sensitivity of the fits to κ, as illustrated in Fig. 10. κ is seen to increase with applied field. The open squares at $H=H_c$ and $H=H_{c3}$ are derived from Eq. (4) and Eq. (1), respectively, with $\lambda_{\text{eff}}=\lambda=39$ nm, $H_c=6.1\times10^4$ A/m (765 Oe), and $H_{c3}=8.1\times10^4$ A/m (1020 Oe) as determined experimentally. The error bars on the latter two κ values derive from the experimental uncertainties in λ, H_c, and H_{c3}.

A/m (765±10 Oe). Assuming the Gorter-Casimir temperature dependence, $H_c(T)=H_c(0)[1-(T/T_c)^2]$, which is applicable to within a few percent for lead,[25] we estimate the critical field at absolute zero to be $H_c(0)=(6.4\pm0.1)\times10^4$ A/m (804±13). This result is in excellent agreement with the accepted value,[25,26] $(6.39)\times10^4$ A/m (803 Oe) for bulk samples of lead.

Values of H_{c3}, and hence of κ via Eq. (1), have been reported for lead from a number of experimental techniques. Thermal and electrical conductivity and microwave surface resistance measurements[17] both gave $H_{c3}/H_c=1.35$ at $T=1.5$ K. This ratio corresponds to $\kappa=0.56$ by Eq. (1), which is the same as we have obtained from the ratio of the critical fields. A rather lower κ was inferred indirectly for pure lead by extrapolation of ac susceptibility measurements in a series of lead-bismuth alloys.[27] The extrapolation indicated $H_{c3}/H_c\approx1.0$ at 4.2 K, which is lower than was reported in Refs. 17, where at the same temperature $H_{c3}/H_c\approx1.15$ for pure lead. It is not clear whether this inconsistency simply reflects experimental error, or whether there is a more fundamental problem in the extrapolation of critical fields from dirty to pure superconductors.

The penetration depth for pure lead has been measured on many occasions, and by a number of different techniques.[28–36] The various results are collected together in Table I. We will not attempt to present a detailed critique of each of the methods, but we would like to dwell briefly on the large discrepancies evident in Table I. This discord reflects the basic problem common to all techniques, namely that of relating the experimentally measured quantity to the actual value of the bulk penetration depth at absolute zero, $\lambda(0)$.

Aside from PNR, the methods listed in Table I fall into one of two categories: those which seek to determine the absolute value of a physical property which depends on λ (Refs. 28, 29, 30, 32, 34, and 35), and those which only measure changes in a quantity relative to a fixed temperature (Refs. 31, 33, and 36). In principle, a technique in the first category can yield the actual penetration depth, but the reliability of the result depends on the validity of the assumptions implicit in the theory used to convert the measured quantity into a penetration depth, and often on having an accurate knowledge of the sample dimensions. For example, the static magnetization methods (Refs. 29 and 32) determine λ from the total flux penetrating the sample, and assume the form of the induction profile across a film derived from the local GL (London) theory. Similarly, the absolute surface impedance measurements (Refs. 28 and 35) require the absolute reactance in the normal state, which cannot be measured directly.

Methods belonging to the second category are often very precise, but are even more indirect than absolute measurements because they are only sensitive to the temperature variation of λ, and not be λ itself. To analyze such data it is usual to consider temperatures close to T_c, where the penetration depth diverges and the superconductor behaves locally. In the local limit λ is equivalent to λ_L, the London penetration depth, whose temperature variation is accurately known[37] close to T_c. A knowledge of $d\lambda_L/dT$ near T_c, together with the size and temperature variation of the energy gap $2\Delta(T)$, yields $\lambda_L(0)$, which can be converted into $\lambda(0)$ if the BCS coherence length ξ_0 is known. With lead, however, there is a great deal of uncertainty in this procedure. Various different values of the ratio $2\Delta(0)/kT_c$ have been used, ranging from 3.5 to 5.5, and ξ_0 is similarly uncertain from 78 to 129 nm. The problems are exacerbated still further by the likelihood of strong-coupling effects in lead, which would modify the BCS temperature variation of the gap, and the question of whether the quasiparticle scattering at the surface is diffuse or specular. Finally, any measurement that uses a sample whose thickness is less than $\sim10\lambda$ is subject to corrections to account for finite-size and mean-free-path effects to obtain the penetration depth of the bulk pure material.

Although the method of obtaining $\lambda(0)$ by PNR is also indirect to some extent, the problems are different from those described above. If the film is sufficiently thick that size effects are unimportant, which we expect to be true within a few percent for the present sample, and if the applied magnetic field is accurately calibrated, as is confirmed by the value of $H_c(0)$ obtained here, then the uncertainties lie entirely in the characterization of the surface and the assumed form of the decay of induction.

It is difficult to judge how the nonideality of the surface will affect the final value of λ. A model with all the right elements should give a good description of both the spin-dependent reflectivities and the flipping ratios. This appears so in the present experiment, and in that case λ should be determined to the stated accuracy. If some factor has been omitted, however, then there may be systematic errors. As shown earlier, the PNR measurements are most sensitive to the *initial* decay of magnetic induction, and do not respond to deviations from a pure exponential decay that might occur at depths greater than a few λ. In this respect the other methods differ, since they determine λ from the *total* flux penetrating into the sample. As the nonlocal correction to the ex-

TABLE I. Literature results for the penetration depth of lead referred to absolute zero. Only the values for the actual penetration depths, $\lambda(0)$, are given even though in some techniques the measured quantity relates more naturally to the London penetration depth, $\lambda_L(T)$, at temperatures close to T_c.

Technique	$\lambda(0)$/nm	Ref.
Absolute surface impedance	~54	28
Magnetization of thin films	39±3	29
Perpendicular field transition	~44	30
Surface impedance	~48[a]	31
Quantum interference in thin film	51-56	32
Field attenuation in thin film	45.3±8	33
Surface impedance in a field	~42	34
Absolute surface impedance	48±4	35
Inductance	~52.5	36
Polarized neutron reflectometry	39±1	This work

[a]Only $\lambda_L(0)$ is given explicitly in Ref. 31, but the results for $\lambda(T)$ obtained by a strong-coupling calculation are shown graphically in Fig. 1, and the value $\lambda(0)\approx48$ nm cited here has been taken from this graph.

ponential decay is predicted to be very small in lead the distinction between these definitions is expected to be of no consequence here.

As may be seen from Table I, the value $\lambda(0)=39\pm1$ nm reported in this work by PNR is on the low side compared with other experimental results. Theoretical predictions for the penetration depth of lead are scarce, but the weak-coupling calculation by Bardeen and Schrieffer[38] gave $\lambda(0)=48$ nm, and a later calculation by Swihart and Shaw,[39] which took account of strong-coupling through the theory of Nam,[40] reduced this value to 40.6 nm for the case of diffuse scattering. In a previous PNR study,[22] preliminary results on lead and Pb(Bi) alloys were presented that included a set of flipping ratios for a lead sample measured at 4.4 K and in a field of 3.2×10^4 A/m (400 Oe). The data were found to be in fair agreement with a calculation that assumed $\lambda(4.4\ \text{K})=40$ nm, but the precision of the measurement was much less than attained in the present work.

Other PNR studies have met with mixed success regarding the penetration depth of simple materials. The data for niobium[12] yielded $\lambda(0)=41\pm4$ nm, in satisfactory agreement with earlier values, but flipping ratio measurements of high statistical quality from a Pb(Bi) alloy[15] differed significantly from a calculation based on the exponential decay model. In that work it was suggested that nonlocal effects might be responsible for the discrepancy, but this explanation is not borne out by our investigations described here.

Although our PNR measurements from the bulk superconducting phase of lead are consistent with the established notion of an exponential decay of magnetic induction, the surface superconducting layer has been less easy to explain in terms of existing theory. The local GL theory is successful in that it can generate an induction profile to fit the experimental flipping ratios at any particular value of the applied field, as shown in Fig. 11, but it is not able to describe all the measurements between H_c and H_{c3} simultaneously with a single set of parameters. Rather, to use the GL theory we found it necessary to increase κ by approximately 10% from H_c to H_{c3}, which is a significantly larger variation than the precision to which κ is determined from an individual run, as illustrated in Fig. 10.

That the GL theory is only semiquantitative for the surface superconductivity is hardly surprising. Not only is it a local theory, but even in type-II superconductors it is strictly valid only near T_c. For example, sufficiently below T_c the penetration depth λ_{eff} that enters into GL theory is not simply related to the actual penetration depth observed below H_c and, moreover, if κ is to vary with applied field then so must λ_{eff} if Eq. (4) is to be satisfied. Notwithstanding these problems of self-consistency and applicability, the GL theory has provided us with a useful, approximate method to obtain the spatial variation of the surface diamagnetism, and it would be interesting to see whether the empirical use of GL theory with a κ parameter that increases with H works for other materials too, and also whether it has any foundation within a proper nonlocal theory of the surface superconducting layer.

VI. CONCLUSIONS

The experiments reported here have been informative both in respect of the technique of PNR and also for the understanding of magnetic-field profiles in nonlocal superconductors. We have found PNR to be very sensitive to the initial rate of decay of magnetic induction, and this feature has enabled us to determine the penetration depth in the bulk superconducting phase of lead with a precision of a few percent. Our value of $\lambda(0)=39\pm1$ nm is somewhat lower than most other experimental determinations. The PNR technique does not appear to be sufficiently sensitive to the fine details of the induction profile to detect the deviations from exponential decay predicted to occur at depths of several times $\lambda(0)$, in type-I superconductors, due to the nonlocal relationship between induced current and field.

We have studied the surface superconducting layer in lead, and found that the induction profile calculated from the Ginzburg-Landau theory provides a useful model of the surface diamagnetism in terms of the phenomenological parameter κ. No one value of κ is able to represent the measurements of the surface diamagnetism over the whole interval from H_c to H_{c3}, but this shortcoming can be overcome if κ is allowed to vary with applied field, while retaining of necessity the GL relationship Eq. (4) between κ, λ_{eff}, and H_c. It is not clear to us whether this purely empirical method has any physical significance or not, but either way we hope that the new experimental dimension brought to surface superconductivity by these PNR measurements will stimulate interest in the development of a truly microscopic theory of the phenomenon.

ACKNOWLEDGMENTS

We are grateful to Dr. J. F. Gregg of the Clarendon Laboratory for advice on the sample preparation, and we would also like to thank Peter Phillips, for technical assistance during the neutron measurements. This work was supported by the Science and Engineering Research Council of Great Britain.

*Also at Department of Physics, University of Warwick, Coventry, CV4 7AL, United Kingdom.

[1]V. L. Ginzburg and L. D. Landau, Zh. Eksp. Teor. Fiz. **20**, 1064 (1950).

[2]D. Saint-James and P. G. de Gennes, Phys. Lett. **7**, 306 (1963).

[3]F. London and H. London, Proc. R. Soc. London Ser. A **149**, 71 (1935).

[4]R. Felici and K. E. Gray, Phys. Rev. B **29**, 6129 (1984).

[5]A. B. Pippard, Proc. R. Soc. London. Ser. A **216**, 547 (1953).

[6]R. Sommerhalder and H. Thomas, Helv. Phys. Acta. **34**, 29

(1961); **34**, 265 (1961).
[7]J. Halbritter, Z. Phys. **243**, 201 (1971).
[8]K. E. Drangeid and R. Sommerhalder, Phys. Rev. Lett. **8**, 467 (1962).
[9]G. P. Felcher, Phys. Rev. B **24**, 1595 (1981).
[10]G. P. Felcher, R. O. Hilleke, R. K. Crawford, J. Haumann, R. Kleb, and G. Ostrowski, Rev. Sci. Instrum. **58**, 609 (1987).
[11]C. F. Majkrzak, Physica B **173**, 75 (1991).
[12]G. P. Felcher, R. T. Kampwirth, K. E. Gray, and R. Felici, Phys. Rev. Lett. **52**, 1539 (1984).
[13]R. Felici, J. Penfold, R. C. Ward, E. Olsi, and C. Matacotta, Nature (London) **329**, 523 (1987).
[14]A. Mansour, R. O. Hilleke, G. P. Felcher, R. B. Laibowitz, P. Chaudari, and S. S. P. Parkin, Physica B **156&157**, 867 (1989).
[15]K. E. Gray, G. P. Felcher, R. T. Kampwirth, and R. Hilleke, Phys. Rev. B **42**, 3971 (1990).
[16]B. Rosenblum and M. Cardona, Phys. Lett. **9**, 220 (1964).
[17]B. Rosenblum and M. Cardona, Phys. Lett. **13**, 33 (1964); T. Seidel and H. Meissner, *ibid.* **17**, 100 (1965).
[18]J. Penfold, R. C. Ward, and W. G. Williams, J. Phys. E **20**, 1411 (1987).
[19]R. Felici, J. Penfold, R. C. Ward, and W. G. Williams, Appl. Phys. A **45**, 169 (1988).
[20]M. Born and E. Wolf, *Principles of Optics* (Pergamon, Oxford, 1975).
[21]L. Névot and P. Croce, Rev. Phys. Appl. **15**, 761 (1980).
[22]G. P. Felcher, R. Felici, R. T. Kampwirth, and K. E. Gray, J. Appl. Phys. **57**, 3789 (1985).
[23]T. B. Light, J. M. Eldridge, J. W. Matthews, and J. H. Greiner, J. Appl. Phys. **46**, 1489 (1975).
[24]M. Tinkham, *Introduction to Superconductivity* (McGraw-Hill, New York, 1975).
[25]D. L. Decker, D. E. Mapother, and R. W. Shaw, Phys. Rev. **112**, 1888 (1958).
[26]See, e.g., E. A. Lynton, *Superconductivity,* 3rd ed. (Methuen, London, 1969).
[27]M. Strongin, A. Paskin, D. G. Schweitzer, O. F. Kammerer, and P. P. Craig, Phys. Rev. Lett. **12**, 442 (1964).
[28]I Šimon, Phys. Rev. **77**, 384 (1950).
[29]J. M. Lock, Proc. R. Soc. London, Ser. A **208**, 391 (1951).
[30]G. D. Cody and R. E. Miller, Phys. Rev. **173**, 481 (1968).
[31]R. F. Gasparovic and W. L. McLean, Phys. Rev. B **2**, 2519 (1970).
[32]G. E. Peabody and R. Meservey, Phys. Rev. B **6**, 2579 (1972).
[33]H. R. Kerchner and D. M. Ginsberg, Phys. Rev. B **10**, 1916 (1974).
[34]Y. Onuki, H. Suematsu, and S. Tanuma, J. Phys. Soc. Jpn. **41**, 1313 (1976).
[35]F. F. Mende, A. I. Spitsyn, N. A. Tereshchenko, and O. E. Rudnev, Zh. Tekh. Fiz. **22**, 1916 (1977) [Sov. Phys. Tech. Phys. **22**, 1111 (1977)].
[36]C. Egloff, A. K. Raychaudhuri, and L. Rinderer, J. Low Temp. Phys. **52**, 163 (1983).
[37]P. B. Miller, Phys. Rev. **113**, 1209 (1959).
[38]J. Bardeen and J. R. Schrieffer, in *Progress in Low Temperature Physics,* edited by C. J. Gorter (North-Holland, Amsterdam, 1961), Vol. 3.
[39]J. C. Swihart and W. Shaw, Physica **55**, 678 (1971).
[40]S. B. Nam, Phys. Rev. **156**, 470 (1967); **156**, 487 (1967).